Strength and Microstructural Developments in Magnesia-GGBS Stabilised Biochar-Sequestered Acid Sulphate Soil

Xue Le[1] and Asadul Haque[2]

[1]Keller Pty Ltd, 62 Mills Road, Braeside, VIC 3195, Australia; email: xue.le@keller.com.au; telephone: +61 3 9590 2600
[2]Department of Civil Engineering, Monash University, Melbourne, VIC 3800, Australia; email: asadul.haque@monash,edu

ABSTRACT

This study assessed the effectiveness of magnesia (MgO) and ground granulated blast-furnace slag (GGBS) in improving the strength of acid sulphate soil (ASS) and the feasibility of sequestering biochar carbon in stabilised ASS. To fulfil the objective of this study, ASS was treated with reactive MgO at 5 to 15%, GGBS at 10 to 20% and biochar at 10%. A range of testings, including pH, uniaxial compressive strength (UCS) test, scanning electron microscopy (SEM) and X-ray diffraction (XRD) analysis, was carried out to investigate strength and microstructural development of the treated ASS over a 180-day curing period. The results of this study showed that MgO-activated GGBS could effectively improve the strength of ASS with an optimum MgO to GGBS ratio of 1:4. Inclusion of biochar can lead to a slight reduction of approximately 10% in strength development of the MgO-GGBS treated ASS. The reduction is due to the porous structure of biochar.

Keywords: acid sulphate soil, soil stabilisation, MgO, GGBS, UCS, carbon sequestration

1 INTRODUCTION

In Australia, there are extensive deposits of acid sulphate soils (ASS), with some 95,000 km^2 (Fitzpatrick et al., 2008) underlying coastal areas. ASS in Australia usually has low strength and high compressibility. To improve the strength of ASS, Portland cement (PC) is commonly used; however, manufacturing PC generates a large amount of CO_2 emissions (0.95 t of CO_2/t of PC) (Yi et al., 2014). In order to reduce the carbon footprint, some industrial by-products, such as ground granulated blastfurnace slag (GGBS) and fly ash, have been adopted as supplementary additives. These supplements are latent-hydraulic materials which typically require alkaline activators to promote their hydration reaction. Recently, reactive magnesia (MgO) has been proposed as a more carbon-effective alternative (0.35 t CO_2/t reactive MgO) to PC in soil stabilisation (Jegandan et al., 2010, Yi et al., 2012); however, its performance in stabilisation of ASS requires further investigation.

To further incorporate sustainability into geotechnical engineering, the concept of sequestering carbon into urban soils, thus reducing atmospheric CO_2, needs to be considered seriously. One possible technology could be sequestration of carbon with biochar through soil mixing process (Haque et al., 2014). Biochar is an alkaline, recalcitrant and highly carbonaceous material produced from the thermal decomposition of biomass (e.g., green waste) (Lehmann, 2007, Renforth et al., 2011, Haque et al., 2014); however, to date, there is limited investigation on the engineering benefits and risks of adding biochar into soil stabilisation.

To reduce the CO_2 emission associated with stabilising ASS, this study investigated the effectiveness of MgO and GGBS in improving the strength of ASS and the feasibility of sequestering biochar carbon in stabilised ASS. A range of testings, including pH, uniaxial compressive strength (UCS) test, scanning electron microscopy (SEM) and X-ray diffraction (XRD) analysis, was carried out to investigate strength and microstructural development of the treated ASS over curing periods of up to 180 days.

2 MATERIALS AND METHODS

2.1 CIS and binders

The ASS was collected from the corner of Batman Hill Drive and Brentani Way in Docklands, Melbourne. In geological terminology, the soil is known as Coode Island Silt (Gill, 1967). The ASS had a liquid limit of 69%, plastic index of 46%, and pH of 8.2. The bulk density and specific gravity of the ASS were approximately 1.6 g/cm^3 and 2.54, respectively. The composition of GGBS (from Building Product Supplies, Australia) and reactive magnesium oxide MgO (XLM Magnesia from Causmag, Australia)

used in this study are shown in Table 1. The biochar used in this study was the pyrolysis product of abandoned rail sleepers. The pH of the biochar was 8.3. Before being added to the sample, the biochar was oven dried for 24 hrs and sieved through 425 μm.

Table 1. Mineralogical composition (% by weight) of GGBS and MgO

Material	SiO_2	Al_2O_3	MgO	CaO	Fe_2O_3	SO_3	MnO	Specific gravity
GGBS	35-37	13.5	5.9	41-43	0.3	2.9	0.4	2.83
MgO	1.3	0.3	97.0	1.3	0.2	-	-	3.24

MgO from 5 to 15% and GGBS from 10 to 20% were mixed with ASS to investigate the optimum MgO-GGBS combination. The MgO-GGBS combinations were each split in two and a fixed 10% of biochar was added to one of the sub-samples. All percentages were by weight of dry soil. In total, 18 binder combinations were adopted in this study, i.e., 5M10S0B, 5M15S0B, 5M20S0B, 5M10S10B, 5M15S10B, 5M20S10B, 10M10S0B, 10M15S0B, 10M20S0B, 10M10S10B, 10M15S10B, 10M20S10B, 15M10S0B, 15M15S0B, 15M20S0B, 15M10S10B, 15M15S10B, and 15M20S10B, where M, S and B represent reactive MgO, GGBS and biochar, respectively, while the number represents the percentage of the additive. In addition, control testing of ASS treated with 20% GGBS only was also carried out as a baseline. A water content of 130% by dry weight of ASS and additives was used to prepare the treated ASS samples. The high water content was adopted to ensure good workability and quality of samples.

2.2 Sample preparation

Due to moisture loss during the transportation and storage process, ASS sourced from the construction site was too stiff to be mixed with additives. Thus, the soil was pre-mixed with a good amount of water in a bench-top mixer for half an hour to break up large soil clumps and obtain a homogeneous soil slurry. At the end of mixing, the slurry was covered with plastic film to minimise any interaction between pyrite and air. After standing overnight, the soil slurry was mixed with additives in the dry form. The mixture was then stirred for 15 minutes in a bench-top mixer. Extra water was added during mixing to achieve a total water content of 130%. The mixture was then cast into cylindical PVC moulds in three layers to prepare samples 60 mm in height and 30 mm in diameter. At the end of placement of each layer, a hand vibrator was used to expel any trapped air bubbles. Both ends of the moulds were sealed with plastic sheets to prevent moisture loss. Samples were subsequently placed in a humidity chamber at 19°C and 100% relative humidity until ready for testing. The stabilised ASS samples were demolded after 7, 28, 90 and 180 days of curing.

2.3 Testing procedure

The pH of stabilised ASS was determined using a MW102 pH metre by mixing 1 part of treated ASS with five parts of deionised water (i.e., weight ratio of treated ASS to water=1:5). The strength of the stabilised ASS was determined through UCS testing in triplicates in accordance with ASTM D2166-06 (ASTM, 2006) at a constant displacement rate of 0.5 mm/min. SEM and XRD analyses were also carried out to examine the microstructure and mineralogical changes of the stabilised ASS. Crushed UCS samples were oven dried overnight at 105°C. Soil flakes with a diameter of no more than 2 mm were selected from the fractured surface of the dried UCS samples for the SEM analysis with a JEOL 7001F microscope. For the XRD analysis, the oven dried samples were ground in an agate mortar, sieved through 425 μm, and subsequently mixed with ethanol (99.7%). The samples were further pulverised with a McCrone Micronising Mill for 5 min. The pulverised samples were then placed in a fume hood for at least 24 hrs to thoroughly volatilise excessive ethanol before the XRD analysis. The XRD analysis was carried out with a Bruker D8 Advance X-ray with Cu-Kα radiation of wavelength λ = 1.5418 Å. The scanning was operated at 40 kV input voltage and 25 mA current with a continuous scan mode from 2θ = 3° to 80°, a step size of 0.02° 2θ, and a counting time of 2 s per step.

3 RESULTS AND DISCUSSION

3.1 pH

The pH variations of the various MgO-GGBS stabilised ASS samples are depicted in Figure 1. The initial pH of all samples was generally in the range 11.6 to 11.9. The pH variations of samples with 10% and 15% GGBS were similar. The pH generally dropped to 90 days and remained at a constant level afterwards. Nevertheless, the pH of ASS with 20% GGBS increased slightly for the first 7 days and

dropped sharply afterwards until 28 days. The increase in pH may be due to the higher amount of GGBS undergoing hydration, releasing more hydroxyls to the pore solution. It is noted that regardless of the GGBS content, the pH of the ASS with 5% MgO dropped more significantly during the first 28 days when compared to counterparts with 10% or 15% MgO. The more significant decrease in pH probably resulted from a greater abundance of cementitious reactions, as evidenced by the higher 28-day strength of soils treated with 5% MgO (as discussed in section 3.2).

Despite the MgO and GGBS content, the pH values of soils with biochar were generally close to those of their counterparts without biochar and the trend of the pH variation was also similar. Although it was previously reported that the pH of a soil was elevated from 4.5 to 6 by the addition of 6% biochar (Chintala et al., 2013), in a strongly alkaline (pH>10) environment, it can be considered that biochar has insignificant influence on the pH of the whole system.

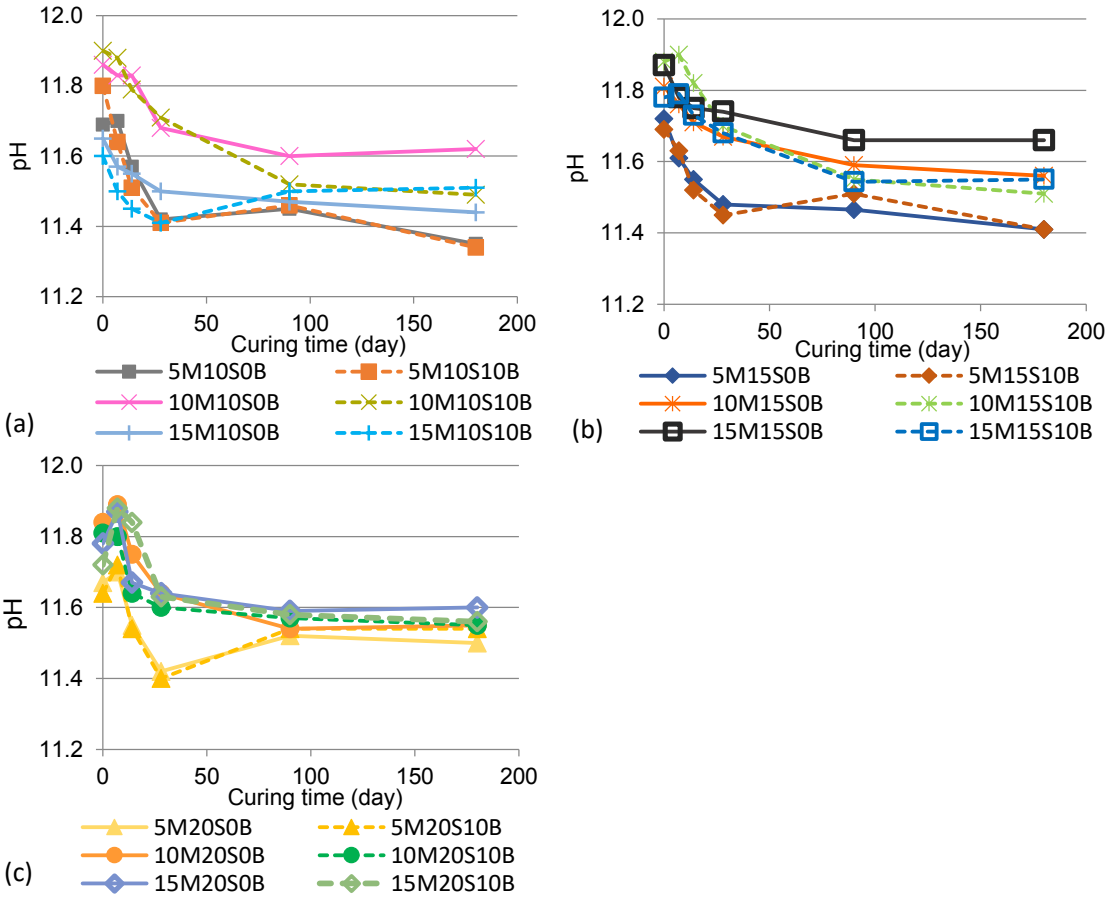

Figure 1. pH of ASS treated with MgO and (a) 10% GGBS, (b) 15% GGBS, and (c) 20% GGBS

3.2 Unconfined compressive strength

The control samples of ASS treated with 20% GGBS only were too soft for UCS testing at the end of a 28-day curing period. At 90 days, the samples registered a strength of 190 kPa. The improvement in the strength is ascribed to the hydration of GGBS. The presence of pyrite and its oxidation products in the mix probably assisted the hydration of the GGBS. Oti et al. (2008) reported that Lower Oxford Clay (LOC) mixed with 20% GGBS alone developed considerable strength at 28 days. They explained that the improvement could be ascribed to the sulphate in the LOC which facilitated the hydration of GGBS.

Figure 2 summarises the UCS results of the MgO-GGBS treated ASS. At 90 days, all samples with 20% GGBS developed more than four-fold of the UCS of the ASS with 20% GGBS only. This implies that MgO significantly enhanced the hydration of GGBS as well as the cementitious reactions. For ASS treated with 20% GGBS, the strength decreased with the increase in MgO content throughout the 6-month curing period. For ASS treated with 10 or 15% GGBS, the strength was also observed to decrease with the increase in MgO content over the first 28 days. However, at 90 and 180 days, increasing MgO

from 5 to 15% had negligible impact on the strength of ASS with 10 to 15% GGBS. It is also evident from Figure 2 that the UCS increases with the increasing GGBS content. The test results suggest that addition of 5% MgO was sufficient to activate up to 20% GGBS in the ASS. It is demonstrated that increasing the MgO content was not necessarily beneficial to the strength development. At higher GGBS content, increasing the MgO amount resulted in the reduction in both short- and long- term strength while at lower GGBS content, the increase in MgO content also decreased the short-term strength. The reduction in the short-term strength may be attributable to the activation limit of reactive MgO to GGBS. It is generally perceived that the rate of hydration of GGBS is faster at higher alkalinity levels (Lothenbach and Gruskovnjak, 2007, Song et al., 2000); however, increasing MgO content from 5% to 15% did not provide a much stronger alkaline environment as shown in the initial pH values (Figure 1). Increasing the MgO to 10 or 15% only resulted in excessive MgO, which was subsequently verified by the XRD analysis. Since the MgO itself did not possess strength or cohesion, the residual MgO only led to a decrease in the short-term strength.

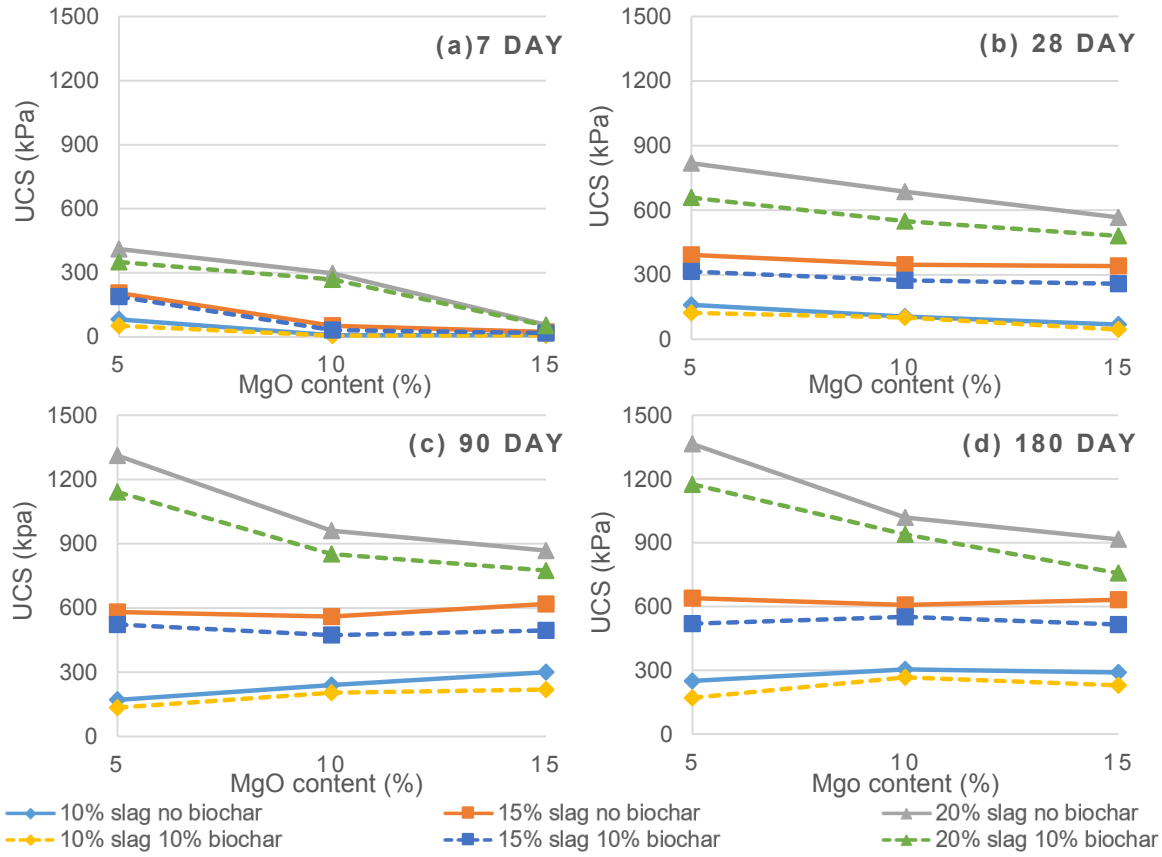

Figure 2. Effects of MgO and GGBS contents on the strength development of ASS at various curing time

It can also be seen from Figure 2 that ASS treated with 10% biochar generally developed slightly lower strength, by approximately 10%, in comparison to the counterparts without biochar. Other than the slight strength reduction, biochar did not influence the trend of strength development. These phenomena show that the biochar probably did not participate in the cementitious reactions but only results in an adverse impact on strength.

3.3 X-Ray diffraction and scanning electron microscopy

The mineralogy of ASS treated with 5% to 15% MgO and 20% GGBS is illustrated in Figure 3. Common minerals including illite, kaolinite, quartz, feldspar and pyrite were identified, reflecting the nature of ASS. The major diagnostic peak of MgO at 2θ= 42.87° appears in the 1-month XRD trace as shown in Figure 3 (a), (b), (e) and (g). The peak of MgO in ASS with 5% MgO has a very low intensity compared to the peaks of MgO in ASS with 10% and 15% MgO, implying more residual MgO in the system with higher MgO contents. The broad peak in the 1-month XRD pattern at 2θ=29.2° is ascribed to the development

of calcium silicate hydrates (C-S-H). The intensity of the peak increased with time from 1 month to 6 months. This correlated to the great increase in strength over the 6 months. It is noted that at each curing period the intensity of C-S-H peak did not differentiate significantly among ASS with different MgO contents. This suggests that there were probably similar amounts of C-S-H formed in ASS, regardless of MgO contents. The XRD results show that increasing the MgO content from 5 to 15% seemed not to promote the formation of C-S-H but only resulted in more residual MgO and brucite. Thus, it can be concluded that 5% MgO was sufficient for activating up to 20% GGBS. Figure 3 (b) and (d) illustrate the mineralogy of ASS with biochar. At both 28 and 90 days, the XRD patterns of ASS with and without biochar were almost identical. This implies that inclusion of biochar neither altered cementitious products nor promoted/hindered the hydration reactions in both short and long term.

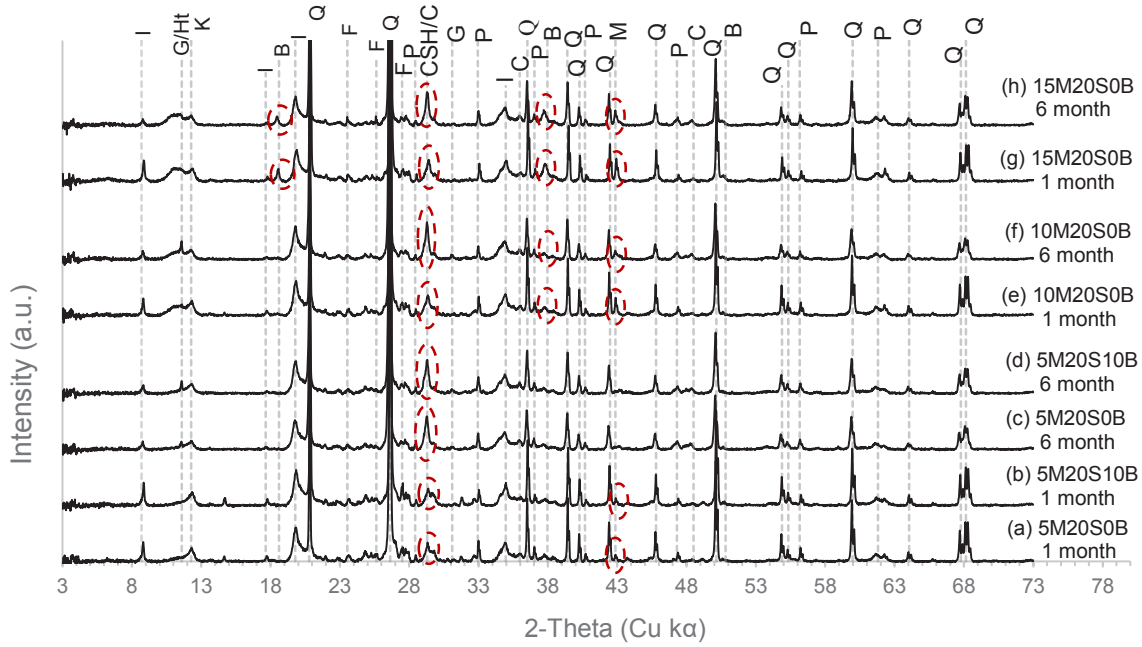

Figure 3. XRD patterns of ASS treated with MgO and 20% GGBS (I-illite, G-gypsum, Ht-hydrotalcite, K-kaolinite, B-brucite, Q-quartz, F-feldspar, C-calcite, P-pyrite, M-MgO)

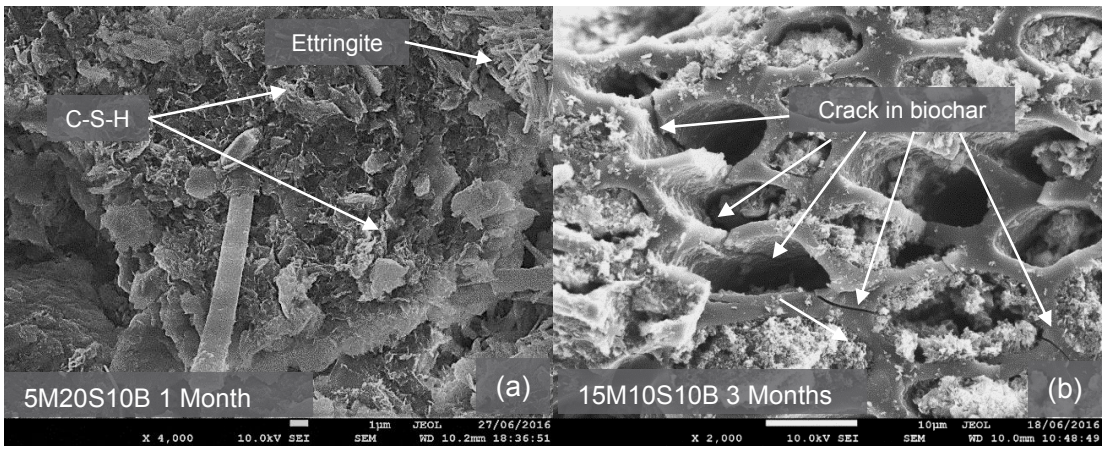

Figure 4. SEM images of ASS treated with MgO-GGBS-biochar binders

Figure illustrates the microstructure of MgO-GGBS-biochar treated ASS. Both C-S-H and ettringite were found in the soil as they are the common hydration products of cementitious reactions. Biochar fragments were found embedded in the ASS-binder matrix with some pores filled with mixtures of soil and cementitious materials. The soil and cementitious materials were also found depositing on part of the biochar surface as shown in Figure 4 (b). Cracks were found propagating across the pores in biochar, particularly in the pores that were left unoccupied or partially occupied as shown in Figure 5 (b). This explains the reason for the lower strength of ASS with biochar. Although biochar did not hinder the

cementitious reactions, cracks tended to propagate across biochar that had unfilled or partially filled pores when subjected to loading. In addition, the smooth surface of biochar with no soil and cementitious material caused lack of bonding between the soil matrix and biochar, which subsequently reduced the cohesion of the treated ASS.

4 CONCLUSION

The pH of all treated ASS test samples underwent a considerable decrease at the early curing stage and the inclusion of biochar had little influence on the pH of the treated ASS. All ASS samples treated with 5 to 15% of MgO and 10 to 20% of GGBS developed signifcant strength over a 180-day curing period, demonstrating that MgO-activated GGBS is an effective binder to improve the strength of ASS. For a GGBS content of 10 to 20%, increasing the MgO content from 5 to 15% generally led to decrease in strength. This implies that 5% MgO is sufficient to activate up to 20% GGBS and thus, the optimum MgO-to-GGBS ratio for strength development of ASS is 1:4 in this study. The XRD and SEM results indicated that the common cementious products of ASS stabilised with MgO-actived GGBS are C-S-H and ettringite.

The XRD and SEM results show that the additon of biochar has negligible impact on the cementitious reactions; however due to its porous structure, inclusion of biochar may lead to a slight reduction in strength. With 10% biochar the reduction is approximately 10%. Nevertheless, inclusion of biochar can offset CO_2 emissions generated by the construction activity and thus, the slight reduction in strength can be justified by the environmental benefits brought by biochar.

5 ACKNOWLEDGEMENTS

The authors appreciate the soil samples provided by Keller Australia. The scholarships provided by Monash University during the first author's postgraduate research work is acknowledged.

REFERENCES

ASTM 2006. Standard Test Method for Unconfined Compressive Strength of Cohesive Soil. Pennsylvania: ASTM International.

FITZPATRICK, R. W. Overview of acid sulfate soil properties, environmental hazards, risk mapping and policy development in Australia. Advances in Regolith. Proceedings of the CRC LEME Regional Regolith Symposia, CRC LEME, Bentley, WA, 2003. 122-125.

CHINTALA, R., MOLLINEDO, J., SCHUMACHER, T. E., MALO, D. D. & JULSON, J. L. 2013. Effect of biochar on chemical properties of acidic soil. Archives of Agronomy and Soil Science, 60, 393-404.

Gill, E.D., 1967, Keilor Excursion No. 40. IN McAndrew J., Marsden M.A.H.(eds) 'Geology excursions handbook for Section C - geology. ANZAAS 39th Congress, Melbourne, January 1967, ANZAAS, 207-208

HAQUE, A., TANG, C. K., ISLAM, S., RANJITH, P. G. & BAI, H. 2014. Biochar Sequestration in Lime-Slag Treated Synthetic Soils: A Green Approach to Ground Improvement. Journal of Materials in Civil Engineering, 06014024-1-06014024-5.

JEGANDAN, S., LISKA, A., OSMAN, A. A.-M. & AL-TABBAA, A. 2010. Sustainable binders for soil stabilisation. Proceedings of the ICE-Ground Improvement, 163, 53-61.

LEHMANN, J. 2007. A handful of carbon. Nature, 447, 143-144.

LOTHENBACH, B. & GRUSKOVNJAK, A. 2007. Hydration of alkali-activated slag: thermodynamic modelling. Advances in Cement Research, vol. 19, pp. 81-92.

OTI, J. E., KINUTHIA, J. M. & BAI, J. 2008. Using GGBS for unfired-clay masonry-bricks. Proceedings of the Institution of Civil Engineers - Construction Materials, 161, 147-155.

RENFORTH, P., EDMONDSON, J., LEAKE, J. R., GASTON, K. J. & MANNING, D. A. C. 2011. Designing a carbon capture function into urban soils. Proceedings of the ICE - Urban Design and Planning [Online], 164. Available: http://www.icevirtuallibrary.com/content/article/10.1680/udap.2011.164.2.121.

SONG, S., SOHN, D., JENNINGS, H. M. & MASON, T. O. 2000. Hydration of alkali-activated ground granulated blast furnace slag. Journal of Materials Science, vol.35, 249-257.

YI, Y., LI, C., LIU, S. & AL-TABBAA, A. 2014. Resistance of MgO-GGBS and CS-GGBS stabilised marine soft clays to sodium sulfate attack. Géotechnique [Online], 64. Available: http://www.icevirtuallibrary.com/content/article/10.1680/geot.14.T.012.

YI, Y., LISKA, M. & AL-TABBAA, A. 2012. Initial Investigation into the Use of GGBS-MgO in Soil Stabilisation. Grouting and Deep Mixing 2012, 444-453.